

Reduction of Ferrylmyoglobin and Ferrylhemoglobin by Nitric Oxide: A Protective Mechanism against Ferryl Hemoprotein-Induced Oxidations[†]

Nikolai V. Gorbunov,^{*,‡} Anatoly N. Osipov,[§] Billy W. Day,^{*,§,||,⊥} Beatriz Zayas-Rivera,[§] Valerian E. Kagan,^{§,||} and Nabil M. Elsayed^{‡,¶}

Department of Respiratory Research, Division of Medicine, Walter Reed Army Institute of Research, Washington, DC 20307, Departments of Environmental & Occupational Health and Pharmaceutical Sciences and Pittsburgh Cancer Institute, University of Pittsburgh, Pittsburgh, Pennsylvania 15238, and Department of Environmental & Occupational Health Sciences, University of California—Los Angeles, Los Angeles, California 90024

Received January 18, 1995; Revised Manuscript Received March 21, 1995[®]

ABSTRACT: The reactions of metmyoglobin (metMb) and methemoglobin (metHb), oxidized to their respective oxoferryl free radical species ($\text{Mb-Fe}^{\text{IV}}=\text{O}/\text{Hb-4Fe}^{\text{IV}}=\text{O}$) by *tert*-butyl hydroperoxide (t-BuOOH), with nitric oxide (NO^\bullet) were studied by a combination of optical, electron spin resonance (ESR), ionspray mass (MS), fluorescence, and chemiluminescence spectrometries to gain insight into the mechanism by which NO^\bullet protects against oxidative injury produced by $\text{Mb-Fe}^{\text{IV}}=\text{O}/\text{Hb-4Fe}^{\text{IV}}=\text{O}$. Oxidation of metMb/metHb by t-BuOOH in a nitrogen atmosphere proceeded via the formation of two protein electrophilic centers, which were heme oxoferryl and the apoprotein radical centered at tyrosine (for the $\text{Mb-Fe}^{\text{IV}}=\text{O}$ form, the *g* value was calculated to be 2.0057), and was accompanied by the formation of t-BuOOH-derived *tert*-butyl(per)oxyl radicals. We hypothesized that NO^\bullet may reduce both oxoferryl and apoprotein free radical electrophilic centers of $\text{Mb-Fe}^{\text{IV}}=\text{O}/\text{Hb-4Fe}^{\text{IV}}=\text{O}$ and eliminate *tert*-butyl(per)oxyl radicals, thus protecting against oxidative damage. We found that NO^\bullet reduced $\text{Mb-Fe}^{\text{IV}}=\text{O}/\text{Hb-4Fe}^{\text{IV}}=\text{O}$ to their respective ferric (met) forms and prevented the following: (i) oxidation of *cis*-parinaric acid (PnA) in liposomes, (ii) oxidation of luminol, and (iii) formation of the *tert*-butyl(per)oxyl adduct with the spin trap DMPO. NO^\bullet eliminated the signals of tyrosyl radical detected by ESR and oxoferryl detected by MS in the reaction of t-BuOOH with metMb. As evidenced by MS of apomyoglobin, this effect was due to the two-electron reduction of $\text{Mb-Fe}^{\text{IV}}=\text{O}$ by NO^\bullet at the oxoferryl center rather than to nitrosylation of the tyrosine residues. Results of our in vitro experiments suggest that NO^\bullet exhibits a potent, targetable antioxidant effect against oxidative damage produced by oxoferryl Mb/Hb.

Myoglobin (Mb)¹ and hemoglobin (Hb) react with alkylhydroperoxides (ROOH) to yield several redox active species, as well as a number of free radical intermediates such as alkylhydroperoxyl (ROO^\bullet), alkylxoxyl (RO^\bullet) and alkyl (R^\bullet) radicals (Trotta et al., 1983; Davies, 1988; Davies, 1989;

Tajima et al., 1990; Maiorino et al., 1994; Hogg et al., 1994). The oxidation of ferric (met) forms of Mb ($\text{Mb-Fe}^{\text{III}}$) and Hb ($\text{Hb-4Fe}^{\text{III}}$) by ROOH is presumed to proceed via two-electron oxidation to give a long-lived oxoferryl ($\text{Fe}^{\text{IV}}=\text{O}$) species, one oxidation equivalent above the ferric state, plus a transient protein radical centered on tyrosine (Tyr 103 in Mb) (King et al., 1963; Davies, 1989; Shiga, & Imaizumi, 1975; Giulivi et al., 1992; Nohl & Stolze, 1993; Choe et al., 1994). Alternatively, the protein radicals ($\text{Mb-Fe}^{\text{IV}}=\text{O}/\text{Hb-4Fe}^{\text{IV}}=\text{O}$) may be directly formed by rapid electron tunneling from Tyr 103 to an initially formed porphyrin radical cation (Tew et al., 1988; Miki et al., 1989; Catalano et al., 1989; Davies, 1991; Giulivi et al., 1992). There is no direct evidence to favor either mechanism of metMb/metHb oxidation. It is, however, suggested from observations that (i) the dioxygen bond of an ROOH can be heterolytically cleaved (Allentoff et al., 1992; Choe et al., 1994; Rao et al., 1994); (ii) Tyr residues are required for the electron transfer to take place during the disproportionation of $\text{Mb-Fe}^{\text{IV}}=\text{O}$ and Mb-Fe^{II} to $\text{Mb-Fe}^{\text{III}}$ (Miki et al., 1989; Giulivi & Davies, 1990); and (iii) both the oxoferryl and protein radical electrophilic centers in $\text{Mb-Fe}^{\text{IV}}=\text{O}/\text{Hb-4Fe}^{\text{IV}}=\text{O}$ molecules can be reversibly reduced by a two-step redox transition (Giulivi et al., 1992).

$\text{Hb-4Fe}^{\text{IV}}=\text{O}$ and $\text{Mb-Fe}^{\text{IV}}=\text{O}$ are extremely potent oxidants (the standard redox potential of the latter is about +1.4 V (Shiga et al., 1975)), whereas the ferrous and ferric

[†] Supported by grants from NSF (MCB-9322598) and the American Heart Association (Pennsylvania Affiliate) to V.E.K. The mass spectral studies were supported by a grant to B.W.D. from the NIH (HL 51469). N.V.G. is a recipient of an NRC Fellowship Award.

^{*} Authors to whom correspondence should be addressed.

[‡] Walter Reed Army Institute of Research.

[§] Department of Environmental & Occupational Health, University of Pittsburgh.

^{||} Pittsburgh Cancer Institute.

[⊥] Department of Pharmaceutical Sciences, University of Pittsburgh.

[¶] Department of Environmental & Occupational Health Sciences, UCLA.

[®] Abstract published in *Advance ACS Abstracts*, May 1, 1995.

¹ Abbreviations: DPH, 1,1-diphenyl-2-picrylhydrazyl; DMPO, 5,5'-dimethyl-1-pyrroline *N*-oxide; DOPC, dioleoyl-L- α -phosphatidylcholine; ESR, electron spin resonance spectroscopy; $\text{Fe}^{\text{IV}}=\text{O}$, oxoferryl; Hb, hemoglobin; $\text{Hb-4Fe}^{\text{III}}$, metHb, ferric (met) form of Hb; Mb, myoglobin; $\text{Mb-Fe}^{\text{III}}$, metMb, ferric (met) form of Mb; MS, ionspray mass spectrometry; NNR, 4,4,5,5-tetramethyl-2-[4-(trimethylammonio)phenyl]-3-oxo-2-imidazolin-1-yloxy methyl sulfate (nitronyl nitroxyl radical); NO^\bullet , nitric oxide; OONO , peroxyxynitrite; PB, sodium phosphate buffer; PnA, 9-*cis*,11-*cis*,13-*cis*,15-*cis*-octadecatetraenoic acid (*cis*-parinaric acid); R^\bullet , alkyl radical; RO^\bullet , alkylxoxyl radical; ROO^\bullet , alkylhydroperoxyl radical; ROOH, alkyl hydroperoxide; t-BuO $^\bullet$, *tert*-butyloxyl radical; t-BuOOH, *tert*-butyl hydroperoxide; $\text{Mb-Fe}^{\text{IV}}=\text{O}$, myoglobin oxoferryl protein radical; $\text{Hb-4Fe}^{\text{IV}}=\text{O}$, hemoglobin oxoferryl protein radical.

forms are essentially inactive as oxidants (King et al., 1963; Van den Berg et al., 1990; Galaris et al., 1989; Mairino et al., 1994; Nohl et al., 1993; Rao et al., 1994). Oxoferryl Mb/Hb species have thus been assumed to be significant contributors to pathological processes that are accompanied by the rupture of erythrocytes and myocytes (Galaris et al., 1989; Van den Berg et al., 1990; Shinar & Rachmilewitz, 1990).

The biological activity of nitric oxide (NO[•]) has received much recent attention (Henry et al., 1991). It has been suggested to be a mediator of the inflammation generated by immunocytes, has the properties of a neurotransmitter in both the central and peripheral nervous systems, and produces relaxation of both airway and vascular smooth muscles (Nathan, 1992; Gaston, 1994). NO[•] also has a salutary role in the prevention of vascular thrombosis (Yao et al., 1992), inflammatory cell-mediated injury (Clancy et al., 1992), and reperfusion injury (Kubels, 1993). The chemical reactions responsible for the biological activities of NO[•] appear to be its coordinate covalent binding to Fe and Cu in metalloproteins and its covalent modification of sulfhydryl groups in proteins (Stamler et al., 1992; Henry et al., 1991, 1993).

NO[•] is soluble in solvents comprising a wide dielectric constant range and can react at gas/H₂O, gas/lipid, and H₂O/lipid interfaces. NO[•] undergoes numerous redox reactions and acts as either a weak oxidizing agent or a reducing agent (the standard redox potential for NO[•] + H₂O/HNO₂ + H⁺ + e⁻ is -0.99 V (Hunsberger, 1974)). It also interacts with some metabolically-formed free radicals to yield nonradical adducts (Beckman et al., 1990; Akaike et al., 1993; Rubbo et al., 1994). One of the most important reactions of NO[•] is its combination with superoxide radical anion to form peroxynitrite (⁻OONO), which can decompose to produce highly reactive hydroxyl radical. The reaction is considered to be responsible for the oxidative damage associated with NO[•] (Beckman et al., 1990). Recently, an antioxidant function of NO[•] against lipid peroxidation in membranes and lipoproteins has been also reported. The antioxidant effects of NO[•] were ascribed to its interactions with lipid-derived radicals (Hogg et al., 1993; Rubo et al., 1994), and/or to the chelation of redox-active metal ions by NO[•] (Kanner et al., 1991; Hogg et al., 1993). Another potential antioxidant mechanism of NO[•], its reduction of oxoferryl species, has not been discussed so far.

In the present investigation, we studied interactions of NO[•] with oxoferryl-hemoproteins. We observed that NO[•] reverted oxoferryl Mb/Hb radicals to their ferric (met) forms and inhibited oxoferryl Mb/Hb radical-catalyzed oxidations of *cis*-parinaric acid and luminol, as well as decomposition of *tert*-butyl hydroperoxide (t-BuOOH) to the *tert*-butoxyl radical (t-BuO[•]). Since no nitrosylation of the apoprotein moiety was detected, we concluded that these antioxidant effects of nitric oxide were due to the reduction of *Mb-Fe^{IV}=O/*Hb-4Fe^{IV}=O to metMb/metHb.

MATERIALS AND METHODS

Reagents. Horse heart Mb, human Hb, *tert*-butyl hydroperoxide, dioleoyl-L- α -phosphatidylcholine (DOPC), 5,5'-dimethyl-1-pyrroline *N*-oxide (DMPO), luminol, deferoxamine mesylate, 1,1-diphenyl-2-picrylhydrazil (DPH), sulfanilamide, *N*-(1-naphthyl)ethylenediamine dihydrochloride, sodium phosphate, and sodium nitrite were purchased from

Sigma Chemical Co. (St. Louis, MO). 9-*cis*,11-*cis*,13-*cis*,15-*cis*-Octadecatetraenoic acid (*cis*-parinaric acid, PnA) was purchased from Molecular Probes, Inc. (Eugene, OR). High-purity gaseous NO[•] and N₂ were obtained from Matheson Co. (Newark, CA). 4,4,5,5-Tetramethyl-2-[4-(trimethylammonio)phenyl]-3-oxo-2-imidazolin-1-yloxy methyl sulfate (nitronyl nitroxyl radical, NNR) was a generous gift from Dr. I. A. Grigor'ev. Gas permeable Teflon tubing (0.8 mm internal diameter, 0.013 mm wall thickness) was purchased from Alpha Wire Co., Elizabeth, NJ.

Preparation of Samples. All buffers were prepared free of metals with deionized H₂O double-distilled from quartz glassware that was stirred overnight in the presence of Chelex-100 ion exchange resin (Bio-Rad, Richmond, CA). Mb and Hb were used after purification through a PD-10 Sephadex G-25 column (Pharmacia LKB, Uppsala, Sweden) in 100 mM sodium phosphate buffer (PB), pH 7.4, or in H₂O.

To produce apoMb, metMb solutions (1 mM, 1 mL) were cooled to 4 °C and then added dropwise to 50 mL of rapidly stirred acetone containing 800 μ L of concentrated HCl held at -20 °C in a NaCl/ice bath. After addition was complete, the solution was allowed to stand for 10 min, and then the precipitated protein was collected by centrifugation (15 min at 3000g). The protein pellets were washed with cold (-20 °C) acidic acetone, dried under a stream of N₂, and then resuspended in 1 mL of either purified H₂O or 2 mM NH₄O₂-CCH₃, pH 7.4, for mass spectrometric analysis.

Solutions of NO[•] were prepared by saturating previously deoxygenated (with N₂ gas) 100 mM PB with NO[•] gas. The concentration of NO[•] in solution was determined (i) by means of the nitronyl nitroxyl radical (NNR) (Joseph et al., 1993) and (ii) by the Griess reaction (Vogel et al., 1969).

Briefly, evaluation of NO[•] concentration with NNR is based on their efficient interaction in aqueous solutions to yield a stable iminonitroxide radical with ESR spectral characteristics measurably different from those of NNR. Aliquots of the NO[•]-containing PB were added to a deoxygenated solution of NNR (250 μ M), and ESR spectra were immediately recorded. The initial 5-line NNR ESR spectrum was converted into a 9-line spectrum of the mixture of NNR with iminonitroxide radicals (Figure 1A, spectra 1 and 2). The ratio of the low-field signals of iminonitroxide (*b*) to the sum of the low-field signals from NNR plus iminonitroxide (*b* + *a*) gave an accurate measure of the amount of NO[•] in solution. The ratio *b*/(*a* + *b*) was proportional to the NO[•] concentration in the buffer.

The complete oxidation of NO[•] was achieved by flushing the solutions with O₂. Solutions (0.5 mL) containing the resulting NO₂⁻ anion were incubated with a 0.5 mL solution containing 1% w/v sulfanilamide in 2.5% v/v H₃PO₄ for 5 min. The resulting diazonium solution was treated with 0.5 mL of 1% w/v naphthylethylenediamine dihydrochloride in 2.5% v/v H₃PO₄ for 10 min. The concentration of NO₂⁻ in the oxygenated solution was determined spectrophotometrically using $\epsilon_{540} = 58\,000\text{ M}^{-1}\text{ cm}^{-1}$ for the azo dye and by comparison to a standard curve generated from solutions containing known amounts of NaNO₂.

Spectrophotometric Measurements. The hemoproteins were mainly in the ferric state after initial purification by gel filtration as determined by UV/VIS spectrophotometry using a Beckman DU 7500 diode array spectrophotometer. The concentrations of metMb ($\epsilon_{630} = 3.5\text{ mM}^{-1}\text{ cm}^{-1}$;

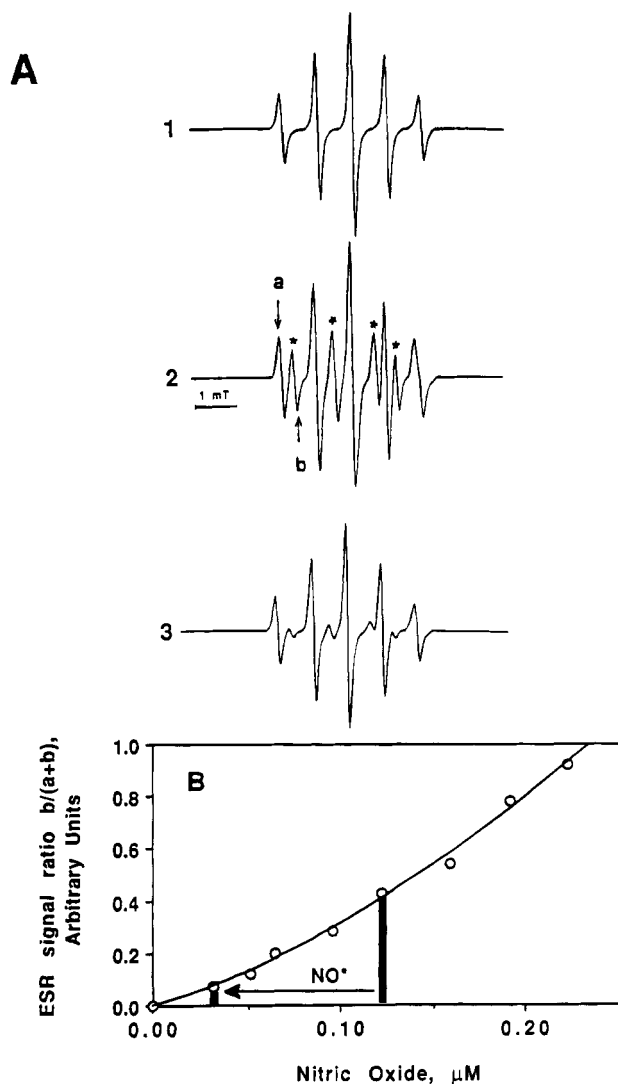


FIGURE 1: (A) ESR spectra of nitronyl nitroxyl radical (NNR) in the presence and in the absence of NO^* . Incubation medium contents: (1) NNR (0.25 mM) in 100 mM phosphate buffer, pH 7.4; (2) NNR (0.25 mM) plus NO^* (0.12 mM) (asterisks indicate the ESR spectral components ascribed to the iminonitroxide radical, (a) the low-field component of NNR spectrum, and (b) the low-field component of iminonitroxide radical); (3) NNR (0.25 mM) plus metHb (0.1 mM), t-BuOOH (10 mM), and NO^* (0.12 mM); note that the ESR spectral components of iminonitroxide radicals are decreased. (B) Dependence of the ratio of the ESR signal of iminonitroxide radical (b) to the sum of the signals of NNR plus iminonitroxide radical ($a + b$) on the concentration of NO^* . The filled bars indicate an example of how the concentration of NO^* changed after addition of metHb and t-BuOOH (consumption of NO^* is shown by the arrow) as measured by the NNR assay, and related to ESR spectra 2 and 3. Each value represents the average of three independent experiments. Data were fit by polynomial regression.

Winterbourn, 1985) and metHb ($\epsilon_{630} = 3.63 \text{ mM}^{-1} \text{ cm}^{-1}$ per heme group; Winterbourn, 1990) were calculated, and the formation/disappearance of oxoferryl Mb/Hb were monitored by recording the absorbance changes at 500 and 630 nm, respectively (Winterbourn, 1985). To perform the spectrophotometric assay, metMb/metHb (100 μM per heme), t-BuOOH (400 μM), and NO^* in 100 mM PB (1.6 mM) were used.

Electron Spin Resonance Spectroscopic (ESR) Measurements. ESR spectra were recorded on a JEOL-RE1X (X-band) spectrometer equipped with 100 kHz modulation.

Samples prepared as described above were transferred to gas-permeable Teflon tubing. The tubing was filled with 30 μL of sample solution under an N_2 or NO^* atmosphere, folded into quarters, and then placed in the quartz tube of the spectrometer. Spectra were obtained at room temperature. ESR settings were as follows: magnetic field magnitude 335.5 mT, microwave power 10 mW and microwave frequency 9.44 GHz, modulation amplitude 1.6 mT, time constant 0.01 s. The ESR response was detected after addition of t-BuOOH (12 mM) to 3 mM metMb in 100 mM PB. Both the g factor and ESR signal intensity were determined relative to external standards, containing Mn^{2+} (in MgO) and DPH. Spectra were simulated using a computer program created by David R. Duling (Laboratory of Molecular Biophysics, National Institute of Environmental Health Sciences, Research Triangle Park, NC).

Parinaric Acid Fluorescence Assay. We used the assay developed by Van den Berg et al. (1990) to evaluate oxidation of *cis*-parinaric acid (PnA) in liposomes by heme iron plus cumene hydroperoxide. Oxidation of PnA in liposomal membranes was measured by the decrease of its fluorescence (Van den Berg et al., 1991) using a Shimadzu RF 5000 U spectrofluorimeter with excitation and emission slits yielding 5 and 10 nm resolution, respectively. Liposomes were prepared from a stock solution of 25.4 mM dioleoyl-L- α -phosphatidylcholine in CHCl_3 (0.16 mL) made 0.25 mM with PnA. The solvent was evaporated under a stream of N_2 on ice. PB (100 mM, pH 7.4, 2.0 mL) was added, and the resulting suspension was sonicated (three 30 s bursts at 65 W) with a Cole-Parmer Instrument Co. 4710 Series Ultrasonicator (Chicago, IL 60648). Liposomes were stored in the dark under N_2 at -80°C . Oxidation experiments were carried out in an N_2 atmosphere. Liposomes (final concentration of lipids 100 μM with integrated 1.0 μM PnA) were introduced into a cuvette containing metMb/metHb (4 μM in heme) and t-BuOOH (16 μM) in 100 mM PB, pH 7.4, with or without 100 μM NO^* . Spectra were obtained in the excitation range of 250–350 nm using an emission wavelength of 415 nm.

Mass Spectral Analyses. Pneumatically-assisted electrospray mass spectra were obtained on a Perkin Elmer/Sciex API I mass spectrometer equipped with an atmospheric pressure ionization source and an articulated IonSpray interface, linked in tandem with glass capillary tubing to a Hewlett Packard 1090 Series II liquid chromatograph equipped with a Hewlett Packard 1040 diode array UV detector. Effluent was monitored by a primary diode array detector monitoring wavelength of 214 nm and by mass spectrometry. The ionspray interface was maintained at 5 kV. High-purity air was used as the nebulizing gas and was maintained at an operating pressure of 40 psi. Analytes were introduced into the ionization source directly from the LC system at 40 mL/min without splitting using 1:1 $\text{H}_2\text{O}-\text{CH}_3\text{OH}$ containing 0.05% $\text{CH}_3\text{CO}_2\text{H}$ and, in some cases, 2 mM $\text{NH}_4\text{O}_2\text{CCH}_3$, as the mobile phase. The presence or absence of NH_4^+ in the mobile phase did not affect results. The orifice voltage was generally set at 90 eV to detect covalent modifications, and at 40 eV to detect coordinate-covalently bound analytes. High-purity N_2 was used as the curtain gas, flowing at 0.6 L/min. The quadrupole was scanned in the appropriate m/z range in 8–11 s/scan at a resolution of m/z 0.1. Protein masses were reconstructed from multiply-charged envelopes of quasimolecular ions by the Fenn

algorithm as implemented by the mass spectrometer manufacturer (Covey et al., 1988), resulting in a resolution of $+1.5$ – 3 amu in the reconstructed mass ranges studied.

In these experiments, the concentrations of reagents were metMb (1 mM, in purified H_2O) and t -BuOOH (4 mM). Solutions of metMb were treated with t -BuOOH for 3 min under an N_2 atmosphere and then exposed to NO^* (bubbled into the solution at $1\text{ cm}^3/\text{min}$). The completed reaction mixture was either frozen in liquid N_2 or filtered through Sephadex G-25 prior to preparation of apoMb. Control solutions were metMb alone, metMb treated with t -BuOOH only, and metMb treated with NO^* only.

Chemiluminescence Assay. Measurements were performed on a Coral Chemiluminescence Analyzer 633 at room temperature. To detect chemiluminescence, reaction mixtures (1 mL in PB, 100 mM, pH 7.4) containing $2\text{ }\mu\text{M}$ metHb were supplemented with $100\text{ }\mu\text{M}$ of luminol. The addition of $100\text{ }\mu\text{M}$ t -BuOOH produced an intense chemiluminescence flash. The emitted light intensity was recorded on a WR 3101 Graphtec, Inc., chart recorder.

Statistical Analysis. Results were obtained from triplicate determinations, expressed as mean \pm SD. Statistical analyses were performed using two-way analysis of variance (ANOVA). A p value of <0.05 was considered significant.

RESULTS

Optical Spectrophotometric Analysis of the Reaction of MetMb/MetHb with t -BuOOH and NO^* . The reaction of excess t -BuOOH ($400\text{ }\mu\text{M}$) with metMb ($100\text{ }\mu\text{M}$) resulted in rapid oxidation of heme Fe^{III} to yield a product with different spectroscopic properties that have been previously ascribed to that of the oxoferryl form of the protein (Figure 2A, spectra 1 and 2). An increase in optical absorbance at 550 and 580 nm indicating $^*Mb-Fe^{IV}=O$ formation was accompanied by a decrease in the absorbance of the metMb component at its maxima of 500 and 630 nm (with the isosbestic point at 614 nm) (Figure 2A, spectrum 2). The exposure of solutions containing $^*Mb-Fe^{IV}=O$ to NO^* under an N_2 atmosphere resulted in regeneration of the metMb spectrum (Figure 2A, spectrum 3). The optical spectral changes observed indicated a redox transition effected by NO^* that was opposite to that by t -BuOOH.

A similar rapid appearance of $^*Hb-4Fe^{IV}=O$ from metHb ($25\text{ }\mu\text{M}$) was also noted upon the reaction of the latter with excess t -BuOOH ($400\text{ }\mu\text{M}$) (Figure 2B, spectra 1 and 2). The absorbance maxima of metHb, 418 (Soret band), 500, and 630 nm, were altered to that of the oxoferryl species, 423 (Soret band, not shown), 543, and 580 nm (Figure 2B, spectra 1 and 2). Oxoferryl hemoglobin produced was stable for at least 30 min in the presence of excess t -BuOOH, as well as after removal of t -BuOOH by gel filtration of the reaction mixture (Figure 2B, spectrum 3). As seen with $^*Mb-Fe^{IV}=O$, the addition of NO^* to the $^*Hb-4Fe^{IV}=O$ solutions resulted in direct redox transition back to metHb, without generation of any observable intermediate states (Figure 2C).

The optical spectra presented on Figure 2B,C illustrate transformation of $^*Mb-Fe^{IV}=O/^*Hb-4Fe^{IV}=O$ into metMb/metHb due to reaction with NO^* in the presence of t -BuOOH. As seen in the spectra obtained, reduction of $^*Mb-Fe^{IV}=O/^*Hb-4Fe^{IV}=O$ by NO^* proceeded without the reductive nitrosylation of metMb/metHb previously reported (Gwost & Caulton, 1973; Alayash et al., 1993).

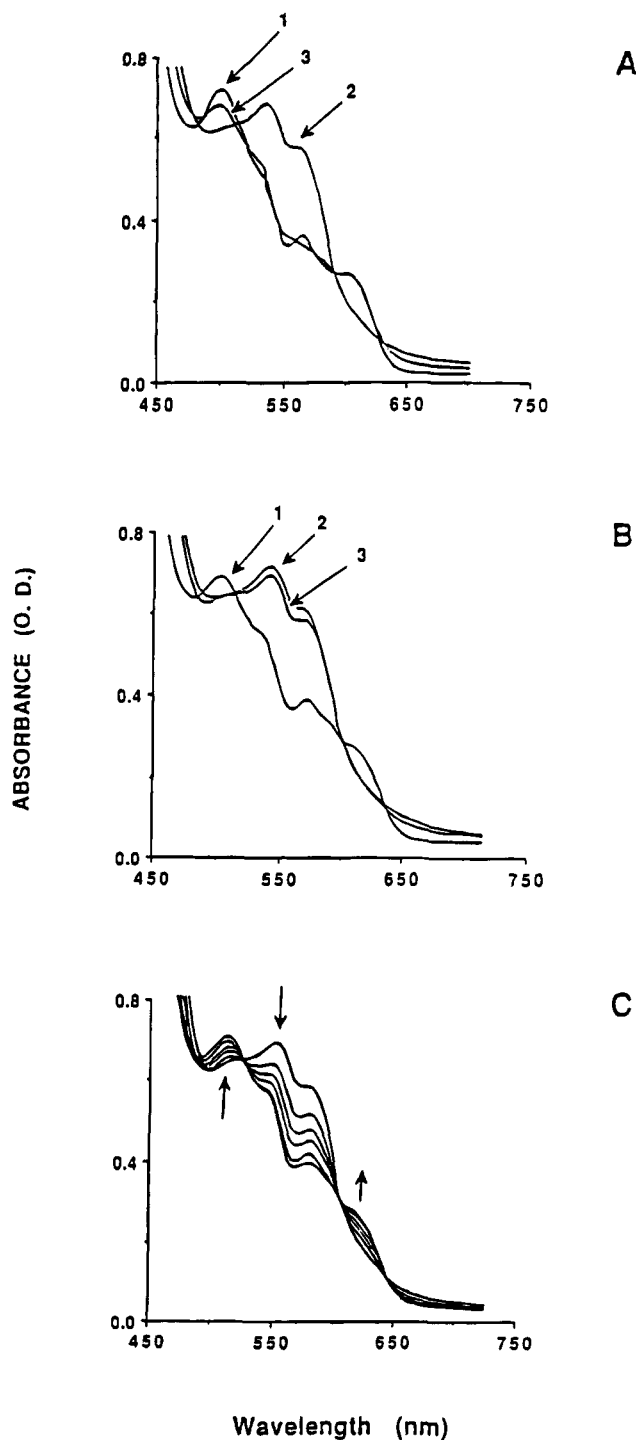


FIGURE 2: Visible absorbance spectra of the reaction products of metMb/metHb with t -BuOOH in the presence and in the absence of NO^* . (A) (1) $100\text{ }\mu\text{M}$ metMb in 100 mM sodium phosphate buffer (pH 7.4). (2) 1 was supplemented with $400\text{ }\mu\text{M}$ t -BuOOH (in an N_2 atmosphere) to produce $^*Mb-Fe^{IV}=O$. (3) After incubation within 5 min, 2 was supplemented with NO^* (1.6 mM) and the spectrum was recorded after 1 min. (B) (1) $25\text{ }\mu\text{M}$ metHb in 100 mM sodium phosphate buffer (pH 7.4). (2) Formation of $^*Hb-4Fe^{IV}=O$ within 5 min after supplementation of $25\text{ }\mu\text{M}$ metHb with $400\text{ }\mu\text{M}$ t -BuOOH. (3) Spectrum 2 after gel filtration of the reaction composition over Sephadex G-25M. (C) $^*Hb-4Fe^{IV}=O$, produced within 5 min after incubation of $25\text{ }\mu\text{M}$ metHb with $400\text{ }\mu\text{M}$ t -BuOOH, was supplemented with 1.6 mM NO^* . Repetitive scans were taken every 15 s. The downward and upward arrows indicate decrease or increase in absorbance at 543 nm ($^*Hb-4Fe^{IV}=O$), and 500 and 630 nm (metHb), respectively.

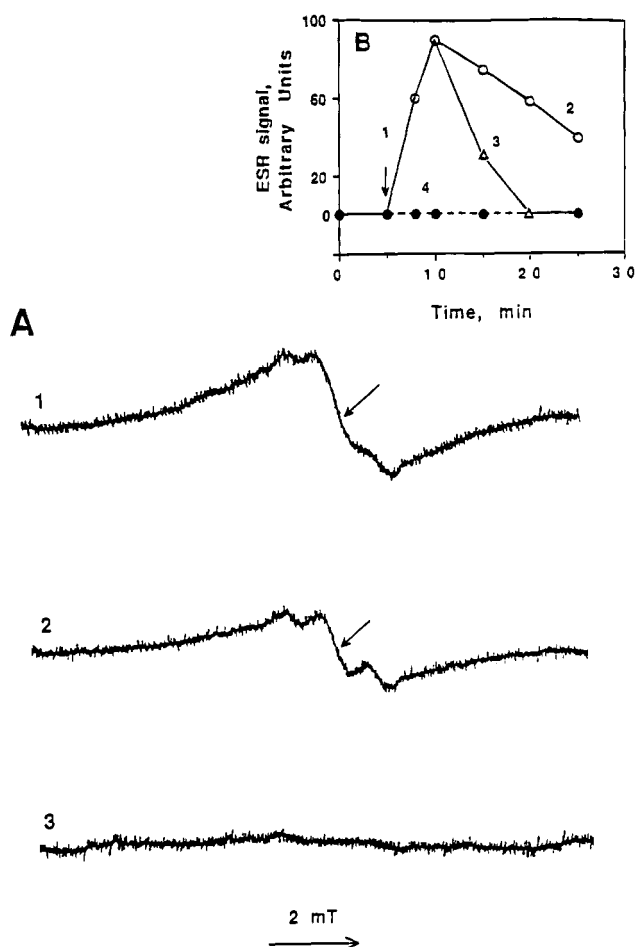


FIGURE 3: (A) ESR spectra of metMb treated with t-BuOOH in the presence and in the absence of NO^{*}. Conditions: (1) metMb (3 mM) in 100 mM sodium phosphate buffer, pH 7.4, and t-BuOOH (12 mM) were incubated in an N₂ atmosphere for 5 min (*g* value at arrow 2.0056); (2) 10 min of incubation (*g* value at arrow 2.0044); (3) 10 min after substitution of N₂ for NO^{*}. (B) Time course of the ESR signal buildup and decay after the addition of t-BuOOH (arrow) to metMb in an N₂ atmosphere (1, 2), and after substitution of N₂ for NO^{*} at the 10th minute (curve 3) or immediately after mixing metMb with t-BuOOH (curve 4). Each value represents the average of three independent experiments.

ESR Spectra Resulting from Interactions of MetMb with t-BuOOH and NO^{*}. The reaction of t-BuOOH (12 mM) with metMb (3 mM) in an N₂ atmosphere resulted in quick generation of a paramagnetic product, with a broad ESR spectrum containing a partially resolved hyperfine structure and broad low- and high-field shoulders, that could be assigned to a protein radical (i.e., [•]Mb-Fe^{IV}=O) centered at tyrosine (Figure 3A, spectrum 1). Indeed, the *g* value at the zero crossing points observed in the ESR spectrum was calculated to be 2.0056, very close to the *g* values earlier reported for the Mb tyrosyl radical (Miki et al., 1989). The profile of the ESR spectrum was also similar to those of tyrosyl radicals in hemoproteins recently reported (Tang, et al., 1993; Nohl & Stolze, 1993).

The magnitude of the [•]Mb-Fe^{IV}=O ESR signal increased within 5 min after addition of t-BuOOH to metMb, after which the decay of the radical was observed, resulting in its disappearance within 20 min (Figure 3B, line 1). This was accompanied by both a decrease in the intensity of central-field component of the ESR spectrum and a shift of the *g* factor value from 2.0056 to 2.0044. The latter is close to

the *g* value reported for the tyrosyl radical of Mb (Davies, 1990) (Figure 3A, spectrum 2). Neither reagent alone yielded an ESR-detectable signal (Figure 3B). Substitution of N₂ for NO^{*} caused gradual disappearance of the spectrum (Figure 3B, curve 3) that was complete within 10 min (Figure 3A, spectrum 3). In the case of substitution of N₂ for NO^{*} immediately after the addition of t-BuOOH to metHb, we did not observe any ESR signal (Figure 3B, line 4).

Effect of FerrylHb on NO^{*} Concentration Evaluated by NNR Spin Trap. Interaction of ferryl Hb with NO^{*} was also confirmed by measuring the NO^{*} concentration in solution by means of the NNR spin trap. When metHb (0.1 mM) and t-BuOOH (10 mM) were added to NO^{*}-containing PB, the decrease of NO^{*} concentration was quantifiable from the observed changes in the ESR spectra (Figure 1B). The initial NO^{*} concentration of 0.12 mM (in the absence of metHb and t-BuOOH) decreased to 0.03 mM within 30 s upon addition of metHb/t-BuOOH (0.25 mM NNR was added 30 s after addition of metHb/t-BuOOH) (Figure 1B). No reagent added singly affected the concentration of NO^{*} as detected by the NNR assay.

DMPO Spin Trapping. Addition of 10 mM t-BuOOH to the mixture of 0.1 mM metHb with the spin trap DMPO (100 mM) gave two different ESR signals after 1 min of incubation. One of the signals corresponded to DMPOX, with coupling constants of *a*_N = 0.71 mT and *a*_{β^H} = 0.40 mT (Figure 4a). This signal was equivalent to that previously reported (Davies, 1988). The second ESR signal was that of the t-BuO^{*}/DMPO adduct, with coupling constants of *a*_N = 1.47 mT and *a*_{β^H} = 1.60 mT. Computer simulation and superposition of the simulated spectra of t-BuO^{*}/DMPO and DMPOX confirmed the presence of these species (Figure 4e–g). The t-BuO^{*} spin adduct was observed regardless of the inclusion or exclusion of the iron chelator deferoxamine in the reaction mixture, strongly suggesting the involvement of heme iron in the radical-generating reaction. Neither of the products' ESR signals were present when either t-BuOOH or metHb was omitted from the reaction mixture (Figure 4b,c). The magnitude of the t-BuO^{*}/DMPO ESR signal was proportional to the concentration of t-BuOOH when it was present within the range of a 2- to 50-fold molar excess over the concentration of metHb (Figure 5, curve 1).

When NO^{*} (0.16 mM) was introduced into the reaction mixture containing metHb, t-BuOOH, and DMPO, the ESR signal from t-BuO^{*}/DMPO was not observed (Figure 4d). At lower NO^{*} concentrations (0.012–0.05 mM), the magnitude of the t-BuO^{*}/DMPO signal decreased proportionally to the concentration of NO^{*} (Figure 5, curve 2). The effects of NO^{*} on the t-BuO^{*}/DMPO spin adduct could be explained either by a direct reduction of the t-BuO^{*}/DMPO spin adduct by NO^{*} or by the interaction of NO^{*} with [•]Hb-4Fe^{IV}=O, resulting in the blockade of the generation of t-BuO^{*} radicals.

To clarify the mechanism of this inhibitory effect of NO^{*} on metHb + t-BuOOH-dependent formation of the t-BuO^{*}/DMPO spin adducts, a system containing 0.1 mM ferrous iron in place of metHb was employed. When 100 mM DMPO was added a few seconds after mixing of t-BuOOH and Fe^{II}, the reaction of t-BuOOH with Fe^{II} gave an ESR spectrum consisting of two superimposed spin adduct signals, with coupling constants of *a*_N = 1.47 mT, *a*_{β^H} = 1.60 mT for one spectrum and *a*_N = 1.62 mT, *a*_{β^H} = 2.32 mT for the second (Figure 6b). The first signal was assigned to the t-BuO^{*}/DMPO adduct, the other to the CH₃[•]/DMPO spin

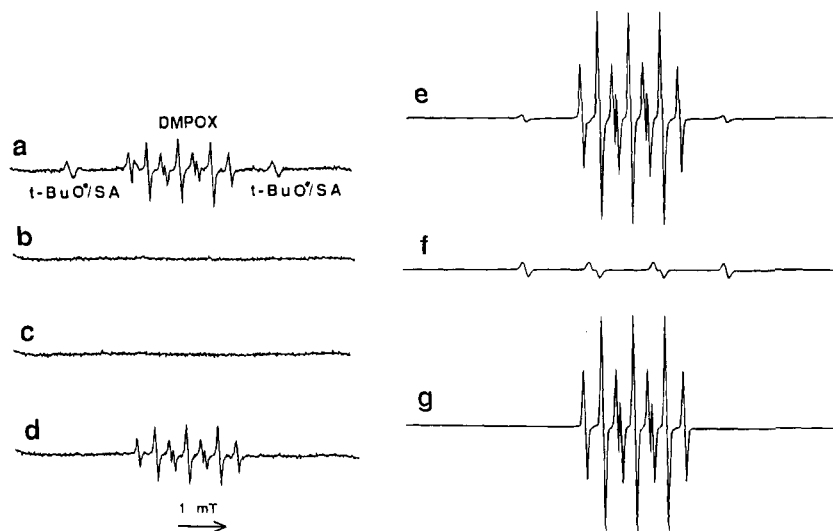


FIGURE 4: Experimentally-obtained and computer-simulated ESR spectra of the spin trap DMPO incubated with metHb and t-BuOOH in the presence and absence of NO[•]. Conditions: 100 mM DMPO in 100 mM phosphate buffer (pH 7.4), was supplemented with 100 μ M metHb and 10 mM t-BuOOH in an N₂ atmosphere. (a) Complete system; superposition of DMPOX signal (central components) and t-BuO[•]/DMPO signal (side components) is evident in the spectrum. (b) Same as (a) except methHb was omitted from the reaction mixture. (c) Same as (a) except t-BuOOH was omitted from the reaction mixture. (d) Same as (a) except N₂ was substituted for NO[•]. (e) Computer-simulated spectrum that is an overlay of both DMPOX and t-BuO[•]/DMPO spectra. (f) Computer-simulated spectrum of t-BuO[•]/DMPO. (g) Computer-simulated spectrum of DMPOX.

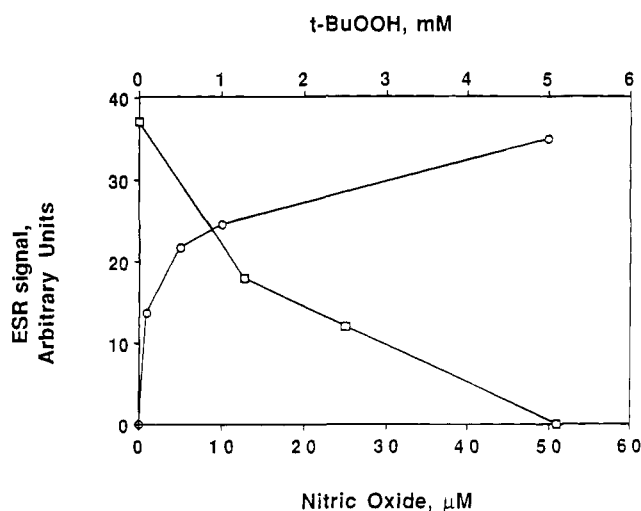


FIGURE 5: Dependence of the ESR signal of the t-BuO[•]/DMPO spin adduct on the concentration of t-BuOOH and NO[•]. Circles: 0.1 mM metHb in 100 mM phosphate buffer, pH 7.4, in an N₂ atmosphere, t-BuOOH as indicated. Squares: 0.1 mM metHb in 100 mM phosphate buffer, pH 7.4, and 10 mM t-BuOOH in an N₂ atmosphere, NO[•] as indicated.

adduct. Our assignments were verified by computer simulations of the spectra (Figure 6e–g). No ESR signals were detected in the absence of either Fe^{II} or t-BuOOH, or when deferoxamine was added to the reaction mixture (Figure 6a–d). When NO[•] was added to the reaction mixture containing Fe^{II} and t-BuOOH, no pronounced changes in the ESR spectra were observed. This suggests that NO[•] did not react with either t-BuOOH-derived radicals or their DMPO spin adducts (Figure 6c). Moreover, the results of this experiment confirmed that the disappearance of the t-BuO[•]/DMPO spin adduct in the metHb/t-BuOOH system was due to the interaction of NO[•] with the electrophilic centers of [•]Hb-4Fe^{IV}=O.

Mass Spectrometric Analysis of the Reaction of MetMb/MetHb with t-BuOOH and NO[•]. The optical and ESR

spectroscopic data suggested that the redox interaction of metMb/metHb with t-BuOOH was accompanied by generation of [•]Mb-Fe^{IV}=O/[•]Hb-4Fe^{IV}=O, as well as free radical products containing fragments of t-BuOOH, that were quenched by NO[•]. To address the apparent anti-radical effect of NO[•], mass spectrometric analyses of metMb, its reaction products with t-BuOOH and NO[•] singly, and the sequential treatment of the protein with t-BuOOH and NO[•] were performed. In these determinations, the crude reaction mixtures as well as the apoprotein and corresponding heme fractions, prepared by precipitation/separation in acidic acetone, were analyzed. Reconstructed mass spectra of metMb obtained at high orifice voltage (90 eV in this case) showed the presence of the apoprotein (16 951 Da in reconstructed spectra) and a very low or undetectable amounts of heme-retaining protein (~17 567 Da) (Figure 7). When spectra were recorded using a lower orifice voltage (40 eV), the heme remained attached to the protein, resulting in a significant amount of signal in the 17 567 (apoprotein + heme) and 17 600 (apoprotein + heme + O₂) Da regions of reconstructed spectra (Konishi & Feng, 1994). Close analysis of the raw spectrum in the heme region (*m/z* 616) additionally revealed the presence of O₂ bound to heme (*m/z* 648) when a lower orifice voltage was used. The presence of molecular oxygen was likely a result of mass spectrometer-induced reduction of Fe^{III} to Fe^{II}, and subsequent attachment of atmospheric O₂.

Reactions of metMb with t-BuOOH resulted in the loss of heme, as detected visually (precipitation of heme in the reaction mixture), by UV analysis, and by mass spectrometry. Evident in mass spectral determinations at high orifice voltage of myoglobin treated with t-BuOOH was formation of Fe^{IV}=O, consistently detected as the heme adduct (*m/z* 632). When the native protein was treated with NO[•], Fe^{IV}=O was not observed, nor were any covalent modifications. When the t-BuOOH-treated protein was treated with NO[•], the Fe^{IV}=O signal disappeared and the resulting spectra were

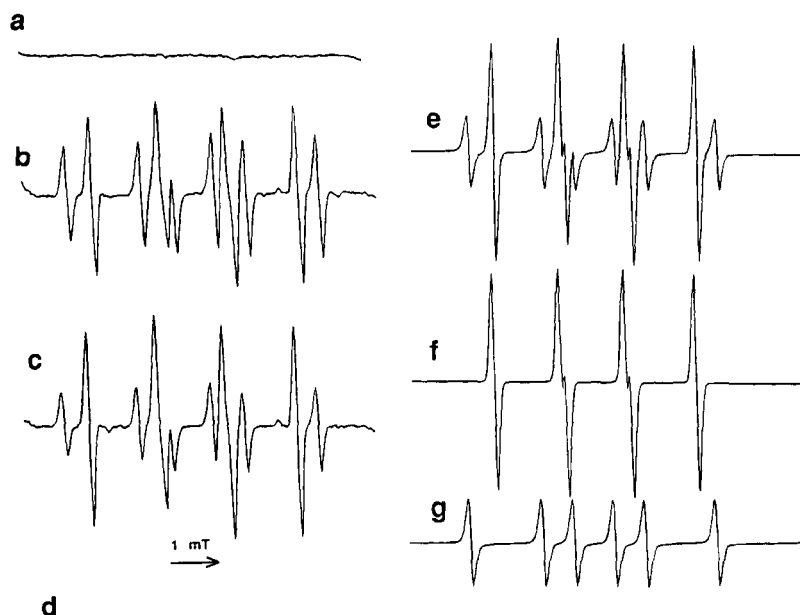


FIGURE 6: Experimentally-obtained and computer-simulated ESR spectra of the spin trap DMPO incubated with Fe^{II} and $t\text{-BuOOH}$ in the presence and absence of NO^\bullet . Conditions: 100 mM DMPO in 100 mM phosphate buffer, pH 7.4, was supplemented with 100 μM Fe^{II} and 10 mM $t\text{-BuOOH}$ in an N_2 atmosphere (complete system). (a) Complete system except $t\text{-BuOOH}$ was omitted. (b) Complete system; superposition of $t\text{-BuO}^\bullet/\text{DMPO}$ and $\text{CH}_3^\bullet/\text{DMPO}$ signals is evident in the spectrum. (c) Same as (b) except N_2 was substituted for NO^\bullet . (d) Same as (b) except deferoxamine (1 mM) was added. (e) Computer-simulated, superimposed spectra of $t\text{-BuO}^\bullet/\text{DMPO}$ and $\text{CH}_3^\bullet/\text{DMPO}$. (f) Computer-simulated spectrum of $t\text{-BuO}^\bullet/\text{DMPO}$. (g) Computer simulated spectrum of $\text{CH}_3^\bullet/\text{DMPO}$.

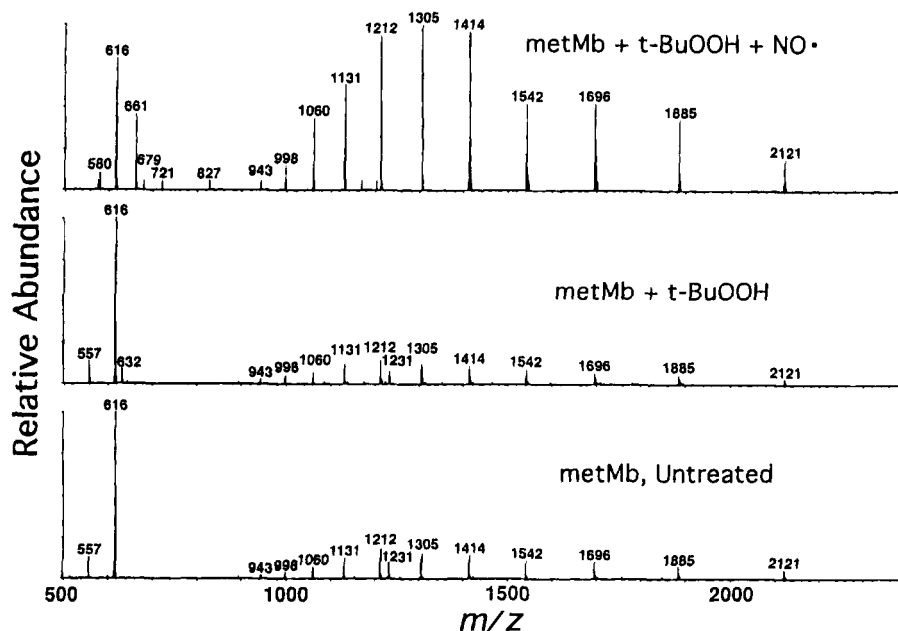


FIGURE 7: Pneumatically-assisted electrospray mass spectra of (from bottom to top) metMb, treated with $t\text{-BuOOH}$ in an N_2 atmosphere, then subsequently with NO^\bullet gas by displacement of the N_2 atmosphere. Note the presence of oxoferryl heme (m/z 632) in the spectrum of the $t\text{-BuOOH}$ -treated protein, and its disappearance upon subsequent treatment with NO^\bullet . The ion signals present between m/z 650 and m/z 900 in the topmost spectrum were not reproducible and are likely unsubtracted solvent and/or electronic noise.

equivalent to those from the untreated and NO^\bullet -treated protein (Figure 7).

Additionally, no evidence for covalent modification of the protein by NO^\bullet was noted. The suspected modifications, either nitrosylation of heme (e.g., m/z 646 that would be detectable in the heme region), nitrosylation of tyrosyl or thyl radicals (e.g., 16 980 Da in the reconstructed spectra of myoglobin or apomyoglobin), or nitrosylation of tyrosine (e.g., 16 996 Da in reconstructed spectra), were not detected in any of the experiments, regardless of the orifice voltage employed in the mass spectral determinations.

Effect of NO^\bullet on the Chemiluminescence of Luminol Induced by MetMb/MetHb plus $t\text{-BuOOH}$. A luminol-dependent chemiluminescence response (due to oxidation of luminol) was produced by the metMb/metHb + $t\text{-BuOOH}$ reaction (Figure 8 A). Similar luminol-dependent chemiluminescence responses were reported in the presence of metHb/ H_2O_2 that, however, developed as a fast spike of chemiluminescence (Nohl & Stolze, 1993). The difference in the time course of the chemiluminescence responses could be due to the different hydroperoxides used ($t\text{-BuOOH}$ vs H_2O_2), as well as to the different concentrations of the

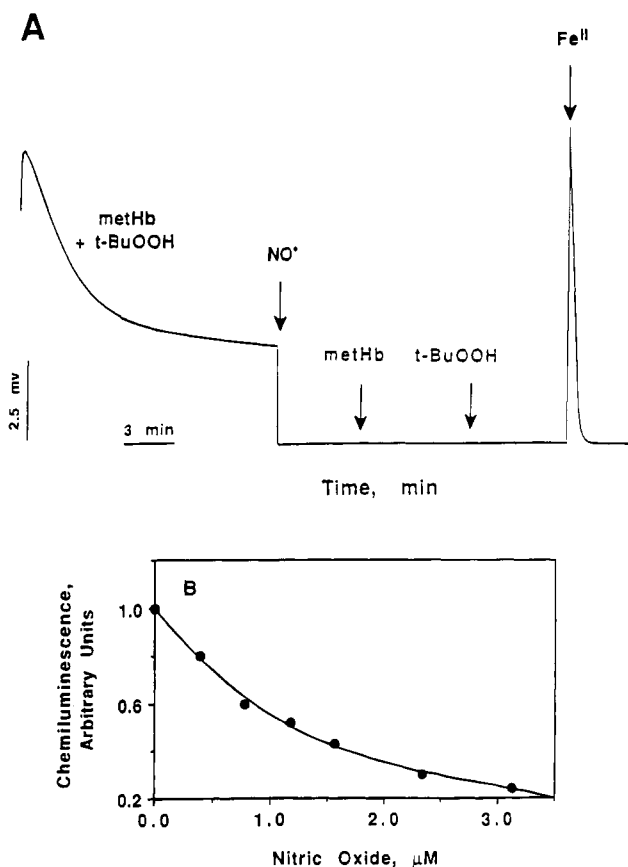


FIGURE 8: (A) Luminol-dependent chemiluminescence response produced by metHb plus t-BuOOH in the presence and absence of NO^{*}. Conditions: 4 μM metHb in 100 mM phosphate buffer, pH 7.4, and 100 μM luminol were supplemented with 100 μM t-BuOOH in an N₂ atmosphere; 25 μM NO^{*} was added after 15 min of incubation. Subsequent additions of metHb (4 μM), t-BuOOH (100 μM), and Fe^{II} (100 μM) are denoted by arrows. (B) Dependence of the chemiluminescence response of luminol in the metHb plus t-BuOOH system 15 min on the concentration of supplied NO^{*}. Conditions: NO^{*} was supplied after incubation of 4 μM metHb in 100 mM phosphate buffer, pH 7.4, with 100 μM luminol and 100 μM t-BuOOH in an N₂ atmosphere. Each value represents the average of three independent experiments. Data were fit by polynomial regression.

hydroperoxides. NO^{*} decreased the light emission in a concentration-dependent manner (Figure 8A,B). After complete elimination of the luminol-dependent chemiluminescence by NO^{*}, repetitive additions of metHb (4 μM) and t-BuOOH (100 μM) in the presence of NO^{*} did not induce a chemiluminescence response (Figure 8A). In contrast, addition of free iron (100 μM) induced a fast spike of chemiluminescence, suggesting that only interaction of NO^{*} with oxoferryl Hb (but not with t-BuO^{*}/t-BuOO^{*} radicals) inhibited oxidation of luminol. Similar results were obtained when metMb was in place of metHb (data not shown).

Inhibition of MetMb/MetHb plus t-BuOOH-Induced Lipid Oxidation by NO^{*}. Incubation of liposomes containing PnA with metMb or metHb in an N₂ atmosphere did not affect the intensity of the PnA fluorescence. We had previously seen that addition of t-BuOOH to metMb/metHb caused generation of both ^{*}Mb-Fe^{IV}=O/^{*}Hb-4Fe^{IV}=O and t-BuO^{*}/t-BuOO^{*} radicals. These products also were responsible for oxidative damage to the liposomes, as evidenced by the decrease in PnA fluorescence (Figure 9, A,B). A 4-fold molar excess of t-BuOOH over that of heme iron caused

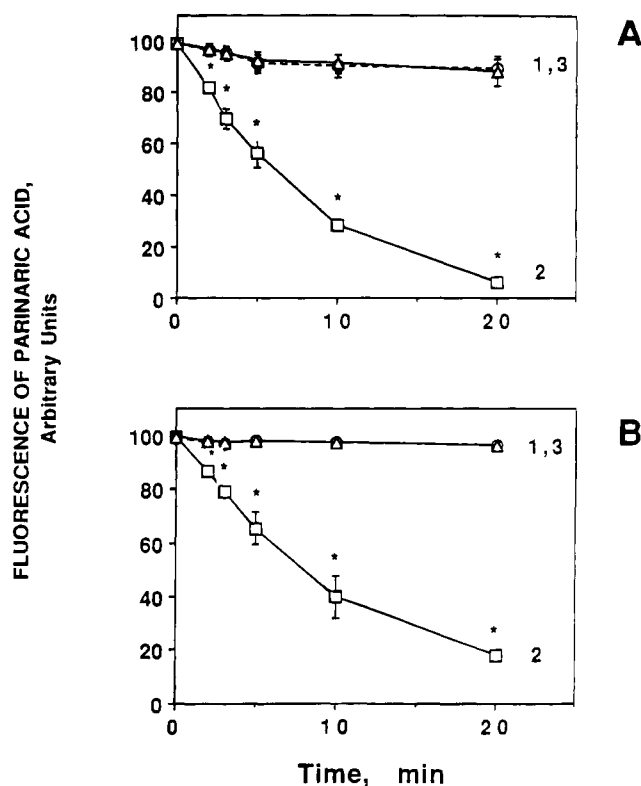


FIGURE 9: Time course of fluorescence of *cis*-parinaric acid in DOPC liposomes incubated with metMb/metHb and t-BuOOH in the presence and absence of NO^{*}. (A) (1) Liposomes (100 μM DOPC and 1 μM PnA) incubated with 4 μM metMb (control). (2) Same as 1, except 16 μM t-BuOOH was added. (3) Same as 2, except 100 μM NO^{*} was added. (B) (1) Liposomes (100 μM DOPC and 1 μM PnA) incubated with 1 μM metHb (control). (2) Same as 1, except 16 μM t-BuOOH was added. (3) Same as 2, except 100 μM NO^{*} was added. Data are means ± SD. Asterisks (*) indicate the data which are significantly different versus control (*p* < 0.01, *n* = 3) as determined by ANOVA with Dunnett's multiple comparisons test.

complete oxidation of PnA within 20 min (Figure 8 A,B). The reaction was completely blocked when 100 μM NO^{*} was added to the system. Neither t-BuOOH alone nor t-BuOOH + NO^{*} caused oxidation of the PnA incorporated into liposomes (data not shown). The inhibitory effect of NO^{*} on PnA oxidation produced by t-BuOOH with metMb/metHb was similar to that previously observed with other reductants, vitamin C and vitamin E (van den Berg et al., 1990), that protected PnA against oxidation produced by ROO^{*} with heme iron.

DISCUSSION

Nitric oxide produced in mammalian cells has proven to act as a mediator of cell communications and as a cytotoxic agent. The cytotoxic effects of NO^{*} are augmented by superoxide anion, due to the formation of peroxynitrite (⁻OONO), a highly potent oxidant capable of generating hydroxyl radicals and NO₂ (Beckman et al., 1990). In addition, the cytotoxicity of NO^{*} released from inflammatory cells may be caused by its suppression of mitochondrial redox function as well as inhibition of ribonucleotide reductase in target cells (Ding et al., 1988; Albina et al., 1991; Hibbs, 1991; Nathan, 1992; Lepoivre, 1992; Henry et al., 1993).

Despite unequivocal evidence that generation of NO^{*} in the presence of superoxide anion produces oxidative damage,

NO^\bullet has also been reported to exert antioxidant effects (Rubbo et al., 1994). This could be due to its scavenging of free radicals to produce nonradical adducts (Rubbo et al., 1994), or to the liganding and inactivation of transient, reactive metal ions in redox catalytic centers by NO^\bullet (Kanner et al., 1991; Hogg, 1993).

The results of the present study suggest that NO^\bullet may function via another protective antioxidant mechanism by reducing oxoferryl Mb/Hb species that may be formed in vivo, e.g., by traumatic tissue damage (Elsayed, 1994) or surgery (Kubels, 1993; Johnson et al., 1991). To address the physicochemical aspects of this protective effect of NO^\bullet against hydroperoxide-activated heme proteins, we studied the formation of, upon reaction with *tert*-butyl hydroperoxide, and decomposition of, upon subsequent reaction with solution-phase NO^\bullet , myoglobin and hemoglobin free radicals by optical, electron spin resonance, ionspray mass, fluorescence, and chemiluminescence spectroscopies. $\text{Mb-Fe}^{\text{IV}}=\text{O}$ and $\text{Hb-4Fe}^{\text{IV}}=\text{O}$ were produced by in vitro reaction of their met forms with t-BuOOH. The products generated in these reactions were shown capable of oxidizing both lipids (*cis*-parinaric acid incorporated into liposomes) and luminol, as well as inducing hemoprotein oxidation and heme release. Treatment of oxoferryl hemoproteins with NO^\bullet was shown to terminate and/or reverse oxidative damage due to reduction of $\text{Mb-Fe}^{\text{IV}}=\text{O}/\text{Hb-4Fe}^{\text{IV}}=\text{O}$ to their respective met forms, but not due to quenching of *tert*-butyl(per)oxyl radicals. These reversal/protective effects were observable only when the full complement of reactants, metMb/metHb, t-BuOOH, and NO^\bullet , were present.

Reduction of Oxoferryl in Heme versus Nitrosylation of the Tyrosyl Radical Hemoproteins by NO^\bullet . To study this apparent antioxidative action of NO^\bullet , we analyzed its reaction with two potential electrophilic centers formed on reaction of metMb/metHb with t-BuOOH: oxoferryl in heme and the Tyr phenoxyl radical of $\text{Mb-Fe}^{\text{IV}}=\text{O}/\text{Hb-4Fe}^{\text{IV}}=\text{O}$. Both optical spectrophotometric and ESR analysis showed that NO^\bullet was capable of reducing $\text{Mb-Fe}^{\text{IV}}=\text{O}/\text{Hb-4Fe}^{\text{IV}}=\text{O}$ to metMb/metHb. There are three hypothetical ways in which NO^\bullet can affect this reduction. One is the independent interaction of NO^\bullet with both oxoferryl and free radical centers, such as the Tyr phenoxyl radical, to produce ferric iron and nitrosyltyrosine (which would presumably be converted to 3-nitrotyrosine), respectively. A second is the nitrosylation of the Tyr phenoxyl radical by NO^\bullet , leading to oxoferryl reduction by nitrosyltyrosine to form the same products in the first postulated mechanism. A third is the direct interaction of NO^\bullet with oxoferryl centers, accompanied by electron tunneling to free radical centers. The first and second mechanisms would produce adducts of NO^\bullet and Mb/Hb, which would be detectable as adducts in the apoprotein. We did not detect covalent modification of apomyoglobin when it was isolated after reaction of metMb with t-BuOOH and NO^\bullet . To assure that covalent products formed from reaction of NO^\bullet with the phenoxyl radical of tyrosine could be detected by pneumatically-assisted electrospray mass spectrometry, we reacted tyrosyltyrosine with the enzyme tyrosinase, and the resulting phenoxyl radical was treated with NO^\bullet . The addition of NO^\bullet caused elimination of the phenoxyl ESR signal, as well as caused formation of covalent adducts as determined by mass spectrometric measurements (data not shown). Full structural characterization of the product from this reaction is underway (Gorbunov, Day,

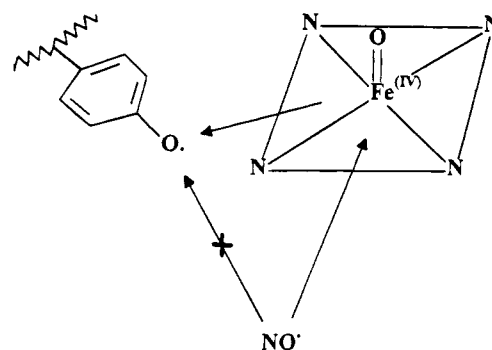


FIGURE 10: Scheme illustrating the proposed mechanism of $\text{Mb-Fe}^{\text{IV}}=\text{O}$ interactions with NO^\bullet . Reduction of heme oxoferryl to ferric form and subsequent intermolecular reduction of the tyrosyl radical are shown.

Zayas-Rivera, and Kagan, unpublished results). Quite the opposite, reaction of NO^\bullet with $\text{Mb-Fe}^{\text{IV}}=\text{O}$ did not produce any ionspray mass spectrometric-detectable covalent adducts on the apoprotein, the heme-bearing protein, nor the heme. These results suggest that the coordination of NO^\bullet with oxoferryl heme iron is the most likely first step of the interaction, rather than protein radical (Tyr phenoxyl) nitrosylation (Figure 10). In addition, metMb/metHb were regenerated from the reaction of $\text{Mb-Fe}^{\text{IV}}=\text{O}/\text{Hb-4Fe}^{\text{IV}}=\text{O}$ as determined by observation of the absorption isosbestic points during the course of the reactions.

It is possible that the reaction of metMb with t-BuOOH resulted in covalent binding of heme to the protein. The reaction of horse heart myoglobin with H_2O_2 has been shown to result in covalent binding of up to 18% of the prosthetic heme group to the protein. Specifically, Tyr 103 has been suggested to become covalently attached to a meso-carbon of heme. Additionally, the chromophore of the protein-bound prosthetic group is very similar to that of heme itself (Catalano et al., 1989). Such a product, sans molecular oxygen, would have a mass of 17 565 Da. This product would not have been detected in our experiments, as its mass would have fallen within our error of detection when the multiply-charged envelopes were reconstructed into mass spectra, especially considering the low amount of signal we observed in this higher Da region. We did not, however, note any such large loss of apomyoglobin signal, after precipitation from the heme fraction, in our measurements. There was a significant loss of heme, but much of it was accounted for as its oxoferryl form. Thus, our results suggest that the oxidation of metMb/metHb by t-BuOOH may be different than that by H_2O_2 .

Mechanism of $\text{Mb-Fe}^{\text{IV}}=\text{O}/\text{Hb-4Fe}^{\text{IV}}=\text{O}$ Reduction by NO^\bullet . It is known that the availability of a free coordination site is a stringent requirement for peroxide activation of ferric heme proteins to their ferryl forms (Tajima et al., 1990; Kanner, 1991). In our experiments, NO^\bullet was effective in the reduction of oxoferryl species obtained after incubation of metMb/metHb with t-BuOOH, suggesting that free radicals consisting of t-BuOOH fragments ligated to the sixth coordination site of the heme ferryl ion do not prevent interaction of the nonbonding electron from NO^\bullet with the unoccupied e_g and t_{2g} orbitals of iron. This would suggest that NO^\bullet can inhibit heme iron catalytic centers after they have coordinately bound t-BuOOH or its decomposition products. Thus, the disappearance of both t-BuOOH-derived free radicals and corresponding DMPO adducts, observed

immediately after addition of NO[•] to the hemoprotein + t-BuOOH couple, can be explained by a mechanism whereby NO[•] interacts with the iron in the heme coordination complex in a redox manner. Indeed, replacement of the met hemoprotein with free Fe^{II} ion in experiments caused production of both t-BuOOH-derived free radicals and luminol chemiluminescence in both the presence and absence of NO[•].

Recently, the pathogenic role of oxoferryl Mb/Hb free radicals produced under ischemia-reperfusion and lung-blast overpressure damage has been discussed (Galaris et al., 1989). Antioxidants such as ascorbate, α -tocopherol, and TROLOX were shown to eliminate the oxidative stress arising from $\text{Mb-Fe}^{\text{IV}}=\text{O}/\text{Hb-4Fe}^{\text{IV}}=\text{O}$ production due to reduction of oxoferryl species to ferric forms (Galaris et al., 1989; Wu et al., 1994; Giulivi et al., 1992). There is also convincing evidence that NO[•] therapy produces a beneficial effect with respect to atherosclerosis, ischemia-reperfusion, acute respiratory distress syndrome, and persistent pulmonary hypertension of the newborn, that can be partially correlated with the antioxidant activity of NO[•] (Schmidt, 1994; Johnson et al., 1991; Kubes, 1993; Hogg et al., 1994; Grover et al., 1994).

It is known that hemoproteins are sinks for NO[•] (Henry et al., 1991). Apparently, NO[•] directly reduces the oxoferryl species to its met form. This points out a potential antioxidant role for NO[•] under conditions of extreme oxidative stress (e.g., inflammation). Ascorbate, which would normally be present in cells at levels high enough to reduce aberrantly-formed oxoferryl proteins, is depleted under conditions of inflammation and traumatic tissue injury. NO[•] produced by inflammatory cells may represent a last line of defense, reducing already damaged iron centers in catalytic or regulatory proteins.

Our in vitro experiments show that NO[•] exhibits a potent, targetable antioxidant effect against the molecular damage catalyzed by oxoferryl Mb/Hb. Studies to elucidate a more complete understanding of the antioxidant action of NO[•] *in vivo*, including the mechanisms of its interaction with well-studied cellular antioxidant systems, now seem to merit further study.

ACKNOWLEDGMENT

Our thanks to Dr. I. A. Grigor'ev Institute of Organic Chemistry, Novosibirsk, Russia, for the generous gift of NNR.

REFERENCES

- Akaike, T., Yoshida, M., Miyamoto, Y., Sato, K., Kohno, M., Sasamoto, K., Miyazaki, K., Ueda, S., & Maeda, H. (1993) *Biochemistry* 32, 827–832.
- Alayash, A. I., Fratanoni, J. C., Bonaventura, C., Bonaventura, J., & Cashon, R. E. (1993) *Arch. Biochem. Biophys.* 303, 332–338.
- Albertini, M., & Clement, M. G. (1994) *Prostaglandins, Leukotrienes Essent. Fatty Acids* 51, 357–362.
- Albina, J. E., Abate, J. A., & Henry, W. L. (1991) *J. Immunol.* 147, 144–148.
- Allentoff, A. J., Bolton, J. L., Wilks, A., Thompson, J. A., & Ortiz de Montellano, P. R. (1992) *J. Am. Chem. Soc.* 114, 9744–9749.
- Beckman, J. S., Beckman, T. W., Chen, J., Marshall, P. A., & Freeman, B. A. (1990) *Proc. Natl. Acad. Sci. U.S.A.* 87, 1620–1624.
- Bult, H., Boeckstaens, G. E., Pelckmans, P. A., Jordaens, F. N., Van Maercke, Y. M., & Herman, A. G. (1990) *Nature (London)* 345, 346–348.
- Catalano, C. E., Choe, Y. S., & Ortiz de Montellano, P. R. (1989) *J. Biol. Chem.* 264, 10534–10541.
- Choe, Y. S., Rao, S. I., & Ortiz de Montellano, P. R. (1994) *Arch. Biochem. Biophys.* 314, 126–131.
- Clancy, R. M., Leszczynska-Pitiak, J., & Abramson, R. B. (1992) *J. Clin. Invest.* 90, 1116–1121.
- Covey, T. R., Bonner, R. F., Shushan, B. I., & Henion, J. (1988) *Rapid Commun. Mass Spectrom.* 2, 249–256.
- Davies, M. J. (1988) *Biochim. Biophys. Acta* 964, 28–35.
- Davies, M. J. (1989) *Free Radical Res. Commun.* 7, 27–32.
- Davies, M. J. (1991) *Biochim. Biophys. Acta* 1077, 86–90.
- Ding, A., Nathan, C. F., & Stuehr, D. J. (1988) *J. Immunol.* 141, 2407–2412.
- Elsayed, N. M., Dodd, K. T., & Fitzpatrick, T. M. (1994) *Am. J. Respir. Crit. Care Med.* 149, A1029.
- Galaris, D., Edy, L., Arduini, A., Cadenas, E., & Hockstein, P. (1989) *Biochem. Biophys. Res. Commun.* 160, 1162–1168.
- Galaris, D., Sevanian, A., Cadenas, E., & Hockstein, P. (1990) *Arch. Biochem. Biophys.* 28, 163–169.
- Gaston, B., Drazen, J. M., Loscalzo, J., & Stamler, J. S. (1994) *Am. J. Crit. Care Med.* 149, 538–551.
- Giulivi, C., & Davies, K. J. A. (1990) *J. Biol. Chem.* 265, 19453–19460.
- Giulivi, C., Romero, F. J., & Cadenas, E. (1992) *Arch. Biochem. Biophys.* 299, 302–312.
- Grover, E. R., Beale, R., Smithies, M., & Bihari, D. (1994) *Anaesth. Int. Care* 22, 312–313.
- Gwost, D., & Caulton, K. G. (1973) *Inorg. Chem.* 12, 2095–2099.
- Henry, Y., Ducrocq, C., Drapier, J.-C., Servent, D., Pellat, C., & Guissani, A. (1991) *Eur. Biophys. J.* 20, 1–15.
- Henry, Y., Lepoivre, M., Drapier, J.-C., Ducrocq, C., Boucher, J.-L., & Guissani, A. (1993) *FASEB J.* 7, 1124–1133.
- Hibbs, J. B. (1991) *Res. Immunol.* 142, 565–569.
- Hogg, N., Kalyanaraman, B., Joseph, J., Struck, A., & Parthasarathy, S. (1993) *FEBS Lett.* 334, 170–175.
- Hogg, N., Rice-Evans, C., Darley-Usmar, V., Wilson, M. T., Paganga, G., & Dourne, L. (1994) *Arch. Biochem. Biophys.* 314, 39–44.
- Hunsberger, J. F. (1974) in *Handbook of Chemistry and Physics* (Weast, R. C., Ed.) Edition D-121, p 55, CRC Press.
- Johnson, G., Tsao, P. S., & Lefer, A. M. (1991) *Crit. Care Med.* 19, 244–252.
- Joseph, J., Kalyanaraman, B., & Hyde, J. S. (1993) *Biochem. Biophys. Res. Commun.* 192, 926–934.
- Kanner, J., Harel, S., & Granit, R. (1991) *Arch. Biochem. Biophys.* 289, 130–136.
- King, K. N., & Winfield, M. E. (1963) *J. Biol. Chem.* 238, 1520–1528.
- Konishi, Y., & Feng, R. (1994) *Biochemistry* 33, 9706–9711.
- Kubes, P. (1993) *Am. J. Physiol.* 264, G143–G149.
- Kwon, N. S., Stuehr, D. J., & Nathan, C. F. (1991) *J. Exp. Med.* 174, 761–767.
- Lepoivre, M., Fieschi, F., Coves, J., Thelander, L., & Fontecave, M. (1991) *Biochem. Biophys. Res. Commun.* 179, 442–448.
- Lepoivre, M., Flaman, J.-M., & Henry, Y. (1992) *J. Biol. Chem.* 267, 22994–23000.
- Mairorino, M., Ursini, F., & Cadenas, E. (1994) *Free Radical Biol. Med.* 16, 661–667.
- McArthur, C. (1994) *J. Respir. Care Pract.* 7, 29–36.
- Miki, H., Harada, K., Yamazaki, I., Tamura, M., & Watanabe, H. (1989) *Arch. Biochem. Biophys.* 275, 354–362.
- Nathan, C. (1992) *FASEB J.* 6, 3051–3064.
- Nohl, H., & Stölze, K. (1993) *Free Radical Biol. Med.* 15, 257–263.
- Radi, R., Beckman, J. S., Bush, K. M., & Freeman, B. A. (1991) *Arch. Biochem. Biophys.* 288, 481–487.
- Rao, S. I., Wilks, A., Hamberg, M., & Montellano, P. R. (1994) *J. Biol. Chem.* 269, 7210–7216.
- Rosen, G. M., & Rauckman, E. J. (1980) *Mol. Pharmacol.* 17, 233–238.
- Rubbo, H., Radi, R., Trujillo, M., Telleri, R., Kalyanaraman, B., Barnes, S., Kirk, M., & Freeman, B. A. (1994) *J. Biol. Chem.* 269, 26066–26075.
- Schmidt, J. M. (1994) *J. Respir. Care Pract.* 7, 37–44.
- Shiga, T., & Imaizumi, K. (1975) *Arch. Biochem. Biophys.* 167, 469–479.

- Shinar, E., & Rachmilewitz, E. A. (1990) *Semin. Hematol.* 27, 70–73.
- Stamler, J. S., Singel, D. J., & Loscalzo, J. (1992) *Science* 258, 1898–1902.
- Tajima, K., Shigamatsu, M., Jinno, J., Kawano, Y., Mikami, K., Ishizu, K., & Ohya-Nishiguchi, H. (1990) *Biochem. Biophys. Res. Commun.* 166, 924–930.
- Tang, X.-S., Chisholm, D. A., Dismukes, G. Ch., Brudvig, G. W., & Diner, B. A. (1993) *Biochemistry* 32, 13742–13748.
- Trotta, R. J., Sullivan, S. G., & Stern, A. (1983) *Biochem. J.* 212, 759–772.
- Van den Berg, J. J. M., Kuypers, F. A., Lubin, B. H., Roelofsen, B., & Op den Kamp, J. A. F. (1990) *Chem. Phys. Lipids* 53, 309–320.
- Van den Berg, J. J. M., Kuypers, F. A., Lubin, B. H., Roelofsen, B., & Op den Kamp, J. A. F. (1991) *Free Radical Biol. Med.* 11, 255–261.
- Vogel, A. I. (1969) in *Textbook of Quantitative Inorganic Analysis*, 3rd ed., p 785, Book Society, London.
- Winterbourn, C. C. (1985) in *Handbook of Methods for Oxygen Radical Research* (Greenwald, R. A., Ed.) pp 137–141, CRC Press, Boca Raton, FL.
- Winterbourn, C. C. (1990) in *Methods in Enzymology*, Vol. 186, pp 265–272, Academic Press.
- Wu, F., Altura, B. T., Gao, J., Barbour, R. L., & Altura, B. M. (1994) *Biochim. Biophys. Acta* 1225 (2), 158–164.
- Yao, S. K., Ober, J. C., Krishnaswami, A., Ferguson, J. J., Anderson, H. V., Golino, P., Buja, L., & Willerson, J. T. (1992) *Circulation* 86, 1302–1309.

BI9501141